Int. J. Heat Mass Transfer. Vol. 23, pp. 881–887

0017-9310/80/0601 0881 $02.00/0

CONVECTION IN A POROUS LAYER

P. G. SIMPKINS
Bell Laboratories, Murray Hill, NJ 07974, U.S.A.

and

P. A. BLYTHE
Center for the Application of Mathematics, Lehigh University, Bethlehem, PA 18015, U.S.A.

(*Received* 13 *August* 1979 *and in revised form* 10 *December* 1979)

Abstract—Steady convective motions inside a rectangular cavity filled with a porous material are examined in the large Rayleigh number limit for flows driven by a horizontal temperature gradient. The boundary-layer structure on the side walls is determined using an integral relations approach. This method leads to results for the core mass flux, for the core-temperature gradient and for the heat-transfer characteristics which are in excellent agreement with numerical solutions of the boundary-layer equations.

NOMENCLATURE

$A(\eta)$,	defined by boundary layer profile (Section 4);
A_1, A_2,	constants in boundary layer profile;
a,	constant (see 3.10);
b,	constant (see 3.16);
c,	constant (see 3.17);
F,	similarity profile for w (see 3.8);
G,	similarity profile for T (see 3.6);
g,	acceleration due to gravity;
h,	cavity height;
k,	permeability;
L,	cavity aspect ratio (l/h);
l,	cavity length;
Nu,	Nusselt number;
Nu^*,	modified Nusselt number (see 3.20);
R,	Darcy–Rayleigh number (see 2.5);
T,	temperature;
u, w,	velocity components;
x, z,	Cartesian co-ordinates.

Greek symbols

α,	coefficient of thermal expansion;
$\alpha_i(z)$,	coefficients in equation (4.2);
$\delta(z)$,	boundary layer thickness;
η,	similarity variable (see 3.7);
κ,	thermal diffusivity;
$\lambda(z)$,	see (4.2) and (4.3);
ν,	kinematic viscosity;
ψ,	stream function.

Superscripts

$'$,	dimensional quantity;
$\tilde{}$,	dimensionless quantity.

Subscripts

c, ∞,	core values;
w,	hot wall value.

1. INTRODUCTION

THERMAL convection problems in porous media occur in a broad spectrum of disciplines ranging from chemical engineering to geophysics. Applications include heat insulation by fibrous materials, spreading of pollutants, and convection in the Earth's mantle. A comprehensive review article has been written by Combarnous and Bories [1].

This paper is concerned with natural convection in a rectangular cavity filled with a porous material. The side walls of the cavity are maintained at different temperatures. Both this problem and its Newtonian fluid counterpart have received less attention than the Bénard problem in which the applied temperature gradient is aligned with the gravitational field. For a Newtonian fluid, thermally driven non-aligned flows have been examined over a wide range of Prandtl numbers; this range encompasses the growth of semiconductor materials from the melt [2], atmospheric circulations [3], and flows in oil-filled cavities [4].

Only steady flows at large Rayleigh numbers are considered here. These flows are characterized by a stratified inviscid core surrounded by thin thermal layers on the cavity walls. For the porous problem, and for Newtonian fluids at high Prandtl numbers, the core structure is dominated by the boundary layers on the vertical walls. An analysis of these boundary layers, together with the compatible core structure, was first given by Gill [5] for the Newtonian case. Quantitative details for the core structure were determined by using a modified Oseen approach [6] to integrate the boundary-layer equations in the large Prandtl number limit. Comparison of the results obtained by this technique with numerical solutions of the Boussinesq equations [7, 8] indicated that the approach led to significant errors in the core mass flux and in the core-temperature gradient.

An alternative analytical procedure, based on in-

tegral relations, was recently developed by Blythe and Simpkins [9]. This method gave better agreement with the numerical solutions for large Prandtl numbers, though there was still a discrepancy in the predicted core mass flux. Since the integral method was based on the boundary-layer equations, whereas the numerical work was concerned with the Boussinesq equations, this disagreement may be due to the error in the boundary-layer approximation. The validity of this assertion could be tested by comparing solutions obtained from the integral method with exact solutions of the boundary layer equations, but unfortunately no such exact solutions are available in the large Prandtl number limit. Recently, however, Walker and Homsy [10] gave a numerical solution of the boundary-layer equations for the analogous porous problem. In the present paper solutions of the porous equations are determined using the integral method. Provided that the chosen boundary layer profile exhibits the correct asymptotic behavior (Section 4), it is found that the integral approach gives good agreement with the numerical solutions. Consequently, it does appear that the error in the predicted core mass flux for the large Prandtl number problem is associated with the boundary layer approximation to the Boussinesq equations rather than with the integral method itself. It is of interest to note that the porous problem has also been analyzed by Weber [11] using the Oseen approach, but similar discrepancies between the Oseen solution and the numerical solution, especially for the core mass flux, are again found to exist (Section 5). Recently, Bejan [12, 13] has suggested a possible modification of the Gill-Weber approach; his analysis is discussed in Section 5.

2. THE FLOW STRUCTURE

A steady convection roll is set up within a rectangular cavity, filled with a porous (Darcy) material, by maintaining the vertical boundaries at different temperatures. Subject to the Boussinesq approximation, the continuity, vorticity and energy equations governing the motion can be written in the non-dimensional form

$$\frac{\partial \bar{u}}{\partial \bar{x}} + \frac{\partial \bar{w}}{\partial \bar{z}} = 0, \tag{2.1}$$

$$\frac{\partial \bar{w}}{\partial \bar{x}} - \frac{\partial \bar{u}}{\partial \bar{z}} = R\frac{\partial \bar{T}}{\partial \bar{x}}, \tag{2.2}$$

and

$$\bar{u}\frac{\partial \bar{T}}{\partial \bar{x}} + \bar{w}\frac{\partial \bar{T}}{\partial \bar{z}} = \frac{\partial^2 \bar{T}}{\partial \bar{x}^2} + \frac{\partial^2 \bar{T}}{\partial \bar{z}^2}. \tag{2.3}$$

The dimensionless variables are defined by

$$(u', w') = \frac{\kappa}{h}(\bar{u}, \bar{w}), \quad T' = \frac{h}{l}T'_w\bar{T},$$

$$(x', z') = h(\bar{x}, \bar{z}), \tag{2.4}$$

where (u, w') are the velocity components with respect to the Cartesian co-ordinate system (x', z') with $z' = 0$ on the lower horizontal boundary; l is the cavity length and h is the cavity height. On $x' = l$ the temperature $T' = T'_w$ (>0) and on $x' = 0$, $T' = 0$. Further,

$$R = \frac{k\alpha g T'_w h^2}{\kappa \nu l} \tag{2.5}$$

is a Darcy–Rayleigh number, κ is the thermal diffusivity, k is the permeability, α is the coefficient of thermal expansion, g is the acceleration due to gravity and ν is the kinematic viscosity.

Appropriate boundary conditions on the vertical walls are

$$\left.\begin{aligned} &\bar{u} = \bar{T} = 0 \quad \text{on} \quad \bar{x} = 0, \\ \text{and} \quad &\bar{u} = 0, \quad \bar{T} = L \quad \text{on} \quad \bar{x} = L = l/h. \end{aligned}\right\} \tag{2.6}$$

If the rigid, horizontal boundaries are perfectly insulated

$$\bar{w} = \frac{\partial \bar{T}}{\partial \bar{z}} = 0 \quad \text{on} \quad \bar{z} = 0, 1, \tag{2.7}$$

but for conducting boundaries the thermal condition is replaced by

$$\bar{T} = \bar{x} \quad \text{on} \quad \bar{z} = 0, 1. \tag{2.8}$$

The governing equations, and the above boundary conditions, possess the centro-symmetric properties [5]

$$\left.\begin{aligned} \bar{\psi}(\bar{x}, \bar{z}) &= \bar{\psi}(L - \bar{x}, 1 - \bar{z}), \\ \bar{T}(\bar{x}, \bar{z}) &= L - \bar{T}(L - \bar{x}, 1 - \bar{z}) \end{aligned}\right\} \tag{2.9}$$

where the stream function $\bar{\psi}$ is such that

$$\bar{u} = \frac{\partial \bar{\psi}}{\partial \bar{z}}, \quad \bar{w} = -\frac{\partial \bar{\psi}}{\partial \bar{x}}. \tag{2.10}$$

When the Darcy–Rayleigh number is large the flow is characterized by thin thermal boundary layers adjacent to the vertical walls. In the interior, or core, the horizontal temperature gradient is small and the motion is equivalent to a parallel stratified shear flow with a positive vertical temperature gradient [5, 11].

Near the vertical boundaries there is a local balance between conduction, convection and vorticity. Suitable co-ordinates for the cold-wall boundary layer are

$$\bar{x} = R^{-1/2}x, \quad \bar{z} = z. \tag{2.11}$$

Corresponding scalings for the dependent variables are

$$\left.\begin{aligned} \bar{\psi}(\bar{x}, \bar{z}; R) &= R^{1/2}\psi(x, z; R), \\ \bar{T}(\bar{x}, \bar{z}; R) &= T(x, z; R) \end{aligned}\right\} \tag{2.12}$$

and, to a first approximation, equations (2.1)–(2.3) reduce to

$$\left.\begin{aligned} \frac{\partial u}{\partial x}+\frac{\partial w}{\partial z}&=0,\\ \frac{\partial w}{\partial x}&=\frac{\partial T}{\partial x},\\ u\frac{\partial T}{\partial x}+w\frac{\partial T}{\partial z}&=\frac{\partial^2 T}{\partial x^2} \end{aligned}\right\} \tag{2.13}$$

where $u = \partial\psi/\partial z$, $w = -\partial\psi/\partial x$. Similar results can be obtained for the hot wall, but it is more convenient to use the symmetry conditions (2.9), see Section 3.

Appropriate core variables, compatible with equations (2.12) and (2.13), are

$$\left.\begin{aligned} \bar{\psi}(\bar{x},\bar{z};R)&=R^{1/2}\psi_c(\bar{x},\bar{z};R),\\ \bar{T}(\bar{x},\bar{z};R)&=T_c(\bar{x},\bar{z};R). \end{aligned}\right\} \tag{2.14}$$

Substitution in equations (2.1)–(2.3) shows that the leading approximation to the core solution is of the form [5, 11]

$$T_c = T_c(\bar{z}), \quad \psi_c = \psi_c(\bar{z}). \tag{2.15}$$

Since the core solution must match with the asymptotic behavior, $x \to \infty$, of the boundary-layer solution it follows that

$$\left.\begin{aligned} &T_c(z) = T(\infty, z) = T_\infty(z)\\ \text{and}\\ &\psi_c(z) = \psi(\infty, z) = \psi_\infty(z). \end{aligned}\right\} \tag{2.16}$$

The functions $\psi_\infty(z)$ and $T_\infty(z)$ must be determined by integration of the boundary-layer equations. In order to complete the solution it is also necessary to specify ψ_∞ as $z \to 0, 1$. For this latter condition Gill [5] assumed that the vertical boundary layers empty into the core so that

$$\psi_\infty(0) = \psi_\infty(1) = 0. \tag{2.17}$$

Strictly, the determination of these limiting values requires the solution of the boundary-layer equations for the horizontal surfaces. A horizontal structure, compatible with (2.17), has been outlined by Walker and Homsy [10] for insulated boundaries. In the conducting case the corresponding boundary-layer structure is considerably more complex and a correct analytical treatment has not yet been given. Nevertheless, numerical calculations for the Newtonian problem (see e.g. [7]) indicate that the core solution is not strongly dependent on the thermal characteristics of the horizontal surfaces and it appears that equation (2.17) may also be a suitable condition on the core solution for conducting boundaries. However, the validity of (2.17) even for insulated boundaries has been questioned by a number of authors (see e.g. Quon [8]). An alternative assumption concerning the horizontal boundary conditions has recently been made by Bejan [12, 13] who suggests that the overall vertical energy flux vanishes as $z \to 0, 1$. Some comments on this assertion are made in Section 5.

3. INTEGRAL RELATIONS FOR THE BOUNDARY LAYER

For the boundary-layer equations (2.13) and the matching conditions (2.16) it can be shown that

$$w = T - T_\infty, \tag{3.1}$$

$$\frac{\mathrm{d}}{\mathrm{d}z}\int_0^\infty (T-T_\infty)^2\,\mathrm{d}x - \psi_\infty\frac{\partial T_\infty}{\mathrm{d}z} = -\left.\frac{\partial T}{\partial x}\right|_{x=0} \tag{3.2}$$

and

$$\psi_\infty = -\int_0^\infty (T - T_\infty)\mathrm{d}x. \tag{3.3}$$

On the wall

$$x = 0: \quad T = 0, \quad \frac{\partial^2 T}{\partial x^2} = 0 \quad \text{etc.} \tag{3.4}$$

and

$$\text{as } x \to \infty: \quad T \to T_\infty, \quad \frac{\partial T}{\partial x}, \quad \cdots \to 0. \tag{3.5}$$

The integral relations (3.2) and (3.3) can be satisfied by similarity solutions of the form

$$T = T_\infty(z)G(\eta), \tag{3.6}$$

where

$$\eta = x/\delta(z) \tag{3.7}$$

and $\delta(z)$ is an appropriate boundary-layer thickness. Correspondingly, from (3.1),

$$W = -T_\infty(z)[1 - G(\eta)] = -T_\infty(z)F(\eta). \tag{3.8}$$

At $x = 0$ these solutions can satisfy only the conditions listed in (3.4). Solutions of this type have previously been used to analyze similar convection problems in viscous fluids at high Prandtl numbers [9]. It is straightforward to show that

$$a\frac{\mathrm{d}}{\mathrm{d}z}(T_\infty\psi_\infty) - \psi\frac{\mathrm{d}T_\infty}{\mathrm{d}z} = -b\frac{T_\infty^2}{\psi_\infty} \tag{3.9}$$

where

$$a = \frac{\int_0^\infty F^2(\eta)\mathrm{d}\eta}{\int_0^\infty F(\eta)\mathrm{d}\eta}, \quad b = -F'(0)\int_0^\infty F(\eta)\mathrm{d}\eta. \tag{3.10}$$

Equation (3.9) provides a single relationship between the unknowns ψ_∞ and T_∞ which govern the core structure. A second relationship can be obtained from the boundary-layer solution for the hot wall but, as noted earlier, it is more convenient to use the symmetry conditions (2.9). The aspect ratio L is eliminated from these conditions, and from the core equation (3.9), by the transformation

$$T_\infty \Rightarrow LT_\infty, \quad \psi_\infty \Rightarrow L^{1/2}\psi_\infty. \tag{3.11}$$

Under this transformation (3.9) is invariant and the symmetry properties reduce to

$$T_\infty(z) = 1 - T_\infty(1-z), \quad \psi_\infty(z) = \psi_\infty(1-z). \tag{3.12}$$

From (3.9) and (3.12) it can be shown that

$$(a-1)\psi_\infty(2T_\infty - 1)\frac{dT_\infty}{d\psi_\infty} = aT_\infty(1-T_\infty)$$

and hence

$$\psi_\infty = c[T_\infty(1-T_\infty)]^{(1-a)/a}, \tag{3.13}$$

where c is a constant.

Consequently, from (3.13), if ψ_∞ vanishes on the horizontal boundaries either $T = 0$ or $T = 1$ at $z = 0, 1$. For $dT_\infty/dz > 0$ it is necessary that

$$T_\infty(0) = 0, \quad T_\infty(1) = 1. \tag{3.14}$$

It is easily seen from (3.9) and (3.14) that

$$\frac{dz}{dT_\infty} = \frac{(1-a)c^2}{b}[T_\infty(1-T_\infty)]^{(2-3a)/a}. \tag{3.15}$$

Since $1 > a > 0$ and $b > 0$ (see Section 4), then $dT_\infty/dz > 0$ and (3.14) are appropriate boundary conditions. Hence,

$$z = \frac{\int_0^{T_\infty}[\theta(1-\theta)]^{(2-3a)/a}\,d\theta}{\int_0^1[\theta(1-\theta)^{(2-3a)/a}\,d\theta} = I_{T_\infty}\left[2\left(\frac{1}{a}-1\right),\ 2\left(\frac{1}{a}-1\right)\right] \tag{3.16}$$

where $I_y(p,q)$ denotes the incomplete beta function normalized with respect to the beta function $B(p,q)$, [14]. The constant c is defined by

$$c^{-2} = b^{-1}(1-a)B\left[2\left(\frac{1}{a}-1\right),\ 2\left(\frac{1}{a}-1\right)\right]. \tag{3.17}$$

From the preceding results it is not difficult to show that

$$\psi_\infty\left(\frac{1}{2}\right) = (\psi_\infty)_{\max} = \frac{4^{-\left(\frac{1}{a}-1\right)}b^{1/2}(1-a)^{-1/2}}{B^{1/2}\left[2\left(\frac{1}{a}-1\right),\ 2\left(\frac{1}{a}-1\right)\right]} \tag{3.18}$$

and

$$\left(\frac{dT_\infty}{dz}\right)_{z=1/2} = \left(\frac{dT_\infty}{dz}\right)_{\min} = 4^{(2-3a)/a}B\left[2\left(\frac{1}{a}-1\right),\ 2\left(\frac{1}{a}-1\right)\right]. \tag{3.19}$$

The variation of the mid-cavity temperature gradient with the parameter a is given in Table 1. This gradient appears to have a stronger dependence on a than in the corresponding high Prandtl number problem [9]. Several boundary-layer models for the determination of the parameters a and b are discussed in Section 4.

Table 1. Mid-cavity temperature gradient

a	0.5	0.55	0.6
$\left(\frac{dT_\infty}{dz}\right)_{\min}$	0.667	0.747	0.841

Overall heat-transfer characteristics for the convection cell are usually expressed in terms of the Nusselt number Nu associated with heat flux across a vertical boundary. In terms of the present variables

$$Nu = L^{3/2}R^{1/2}\int_0^1\left(\frac{\partial T}{\partial x}\right)_{x=0}dz$$

or

$$Nu^* = L^{-3/2}R^{-1/2}Nu = (1-a)cB\left[\frac{1}{a}+1,\ \frac{1}{a}-1\right] \tag{3.20}$$

where Nu^* is dependent only on the parameters a and b. Values of Nu^*, and also of $(\psi_\infty)_{\max}$, are presented in Section 5 for various boundary-layer profiles.

4. BOUNDARY LAYER PROFILES

A self-contained theory for the core structure requires the determination of the parameters a and b. Once the boundary-layer profile $F(\eta)$ has been specified these parameters can be obtained from (3.10). The profile is subject to the constraints

$$\left.\begin{aligned} F(0) = 1, \quad F''(0) = 0 \\ \text{and} \\ F(\infty) = F'(\infty) = \cdots = 0. \end{aligned}\right\} \tag{4.1}$$

In addition, from (2.13) and (2.16) it can be shown that the asymptotic decay, $x \to \infty$, of the boundary-layer solution has the form

$$w = \alpha_1(z)e^{-\lambda(z)x} + \alpha_2(z)e^{-2\lambda(z)x} + \cdots \tag{4.2}$$

with

$$\lambda(z) = \frac{1}{2}\left[-\frac{d\psi_\infty}{dz} + \left\{\left(\frac{d\psi_\infty}{dz}\right)^2 + 4\frac{dT_\infty}{dz}\right\}^{1/2}\right]. \tag{4.3}$$

This monotonic decay should be contrasted with the oscillatory behavior which occurs for flows at large Prandtl numbers [5]. In the latter case better agreement with numerical solutions is obtained if the model profile has the appropriate asymptotic form [9]. This also appears to be true for the present porous problem, and three possible model profiles are discussed below.

(a) *Polynomial-exponential profile*

By analogy with the high Prandtl number solution a suitable profile would be of the form $F = A(\eta)e^{-\eta}$. If it is assumed that

$$F(\eta) = (A_1 + A_2\eta)e^{-\eta}$$

the asymptotic limits in (4.1) are automatically satisfied. The conditions at the origin imply that

$$F(\eta) = (1 + \tfrac{1}{2}\eta)e^{-\eta} \tag{4.4}$$

and hence from (3.10)

$$a = 13/24 \approx 0.542, \quad b = 3/4 = 0.75.$$

(b) *Exponential profile*

Although the profile (a) does satisfy conditions (4.1), equation (4.4) is not strictly of the correct asymptotic form. Apart from constant factors, (4.4) implies that $F \sim \eta e^{-\eta}$ rather than $e^{-\eta}$ as $\eta \to \infty$. The rational function

$$F(\eta) = \frac{A_1 e^{-\eta}}{1 + A_2 e^{-\eta}}$$

does have the correct type of limiting behavior and the choice

$$F(\eta) = \frac{2e^{-\eta}}{1 + e^{-\eta}} \tag{4.6}$$

satisfies the conditions at the origin. For this profile

$$a = 2 - (\ln 2)^{-1} \approx 0.557, \quad b = \ln 2 \approx 0.693. \tag{4.7}$$

(c) *Inner-outer model*

Polynomial profiles, with the asymptotic conditions imposed at some finite value of η, are often used in conventional boundary-layer calculations. As noted earlier, it is important that the asymptotic decay has the correct form, though a polynomial profile may provide a better fit near to the wall than either of the cases discussed above. The two layer profile

$$\left.\begin{aligned} F &= 1 - \frac{9}{14}\eta + \frac{1}{14}\eta^3 \quad 0 \le \eta \le 1 \\ &= \frac{3}{7}e^{-(\eta-1)} \qquad\qquad \eta > 1 \end{aligned}\right\} \tag{4.8}$$

satisfies all of the conditions (4.1) and is compatible with (4.2). At $\eta = 1$ the functions F, F', F'' are continuous. It follows from (3.10) that

$$a = \frac{922}{1715} \approx 0.538, \qquad b = \frac{81}{112} \approx 0.723. \tag{4.9}$$

Although there are many profiles which can satisfy the limiting conditions (4.1), the core solution is influenced by the choice of profile only through the parameters a and b. Since the parameter a is defined in terms of integrals across the layer [see (3.10)], the dependence of the overall core structure on the precise form of $F(\eta)$ is relatively weak. There are, however, rational grounds for choosing profile (c). A local power series expansion in x can always be developed near $x = 0$. As $x \to \infty$ the asymptotic behavior is of the form (4.2). If it is assumed that these two expansions overlap (at say $x = \delta$) then, correct to third order in the x-derivatives, the inner and outer solutions do reduce to the forms given in (4.8).

5. RESULTS

Table 2 lists values of $(dT_\infty/dz)_{min}$, $(\psi_\infty)_{max}$ and Nu^* for the profiles discussed in Section 4. Walker and Homsy [10] used a numerical technique to integrate the boundary-layer equations and some of their results are shown, for comparison, in Table 2. Values determined by Weber [11] using the modified Oseen approach are also given in Table 2. The latter method is known to lead to significant errors in the evaluation of the stream function $\psi_\infty(z)$. However, for each of the boundary-layer profiles discussed in Section 4, the present integral approach gives good agreement with the numerical calculations.

It is also of interest to note that in the corresponding high Prandtl number case the integral method overestimates $\psi_\infty(z)$ when compared with numerical solutions of the Boussinesq equations. Since the comparison is made here with a numerical solution of the boundary-layer equations, it appears that the previous discrepancy arose from the inherent error in the boundary layer approximation rather than from the integral relations approach.

Figures 1 and 2 show a detailed comparison of the various theories for the temperature and the stream function respectively. In these figures the calculations for the integral method were based on the two-layer profile which provides a satisfactory fit with available data for the boundary layer structure. Also shown in Fig. 1 are some experimental results for the temperature profile [15]. Although it is clear that all the theories are in reasonable agreement with respect to the temperature distribution, the modified Oseen approach, as in the high Prandtl number limit, significantly overestimates the local mass flux, see Fig. 2. This latter quantity, together with other core quantities, is accurately predicted by the integral method outlined in this paper.

In the present analysis it has been assumed that the

Table 2. Values for the core parameters

	$\left(\frac{dT_\infty}{dz}\right)_{min}$	$(\psi)_{max}$	Nu^*
Walker and Homsy [10]	0.75	0.733	0.51
Weber [3]	0.67	0.87	0.58
Present profile (a)	0.733	0.747	0.521
Present profile (b)	0.760	0.718	0.508
Present profile (c)	0.726	0.734	0.510

vertical boundary layers empty into the core, i.e. $\psi_z(0) = \psi_\infty(1) = 0$. An alternative assumption for the core solution has recently been made by Bejan [12, 13] who suggested that, for insulated boundaries, the overall vertical energy flux vanishes as $z \to 0, 1$. Bejan has extended the analysis of Gill [5] and Weber [11] to incorporate this energy flux constraint which, in the present notation, implies that

$$\psi_z(0) = \psi_z(1) = \psi_e(R/L).$$

For the modified Oseen technique,

$$\psi_e = 0\left[\left(\frac{L}{R}\right)^{1/4}\right] \tag{5.1}$$

as $R/L \to \infty$, but for the integral method it can be shown that

$$\psi_e = 0\left[\left(\frac{L}{R}\right)^{\frac{1-a}{2(3-4a)}}\right]. \tag{5.2}$$

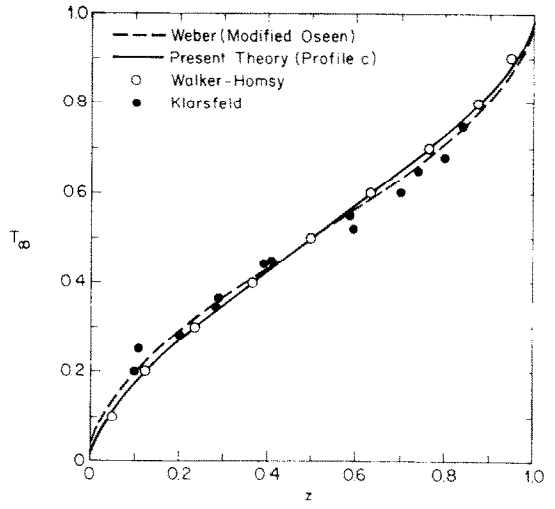

FIG. 1. Temperature profiles in the core.

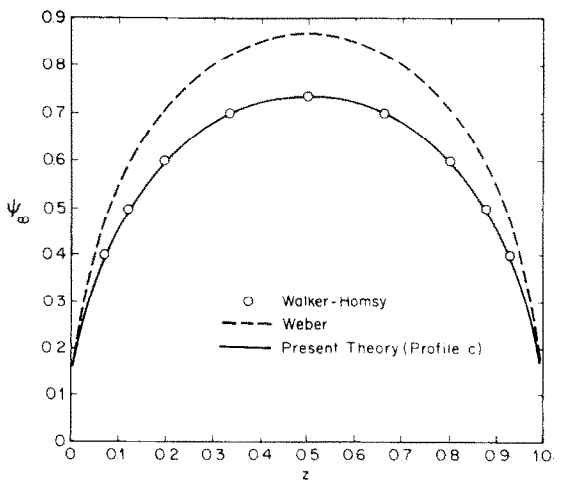

FIG. 2. Core stream function.

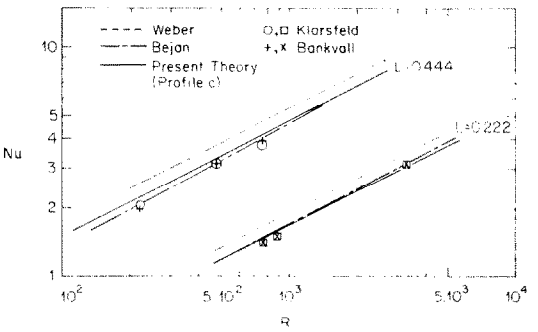

FIG. 3. Predicted heat-transfer characteristics.

Obviously, as $R \to \infty$, these limiting conditions on the core solution again reduce to $\psi_z(0) = \psi_z(1) = 0$.

Experimental results [15] for the Nusselt number, and some numerical calculations for the full equations [16], are shown in Fig. 3 for two different aspect ratios. Included in this figure are predictions from the present analysis and from Bejan's extension of Weber's analysis. The present analysis is represented in the figure by profile (c), though as can be seen from Table 2 the results for Nu using profile (b) are virtually indistinguishable from those associated with (c). Profile (a) leads to results for Nu which are 2% greater than those for profile (c). [It is of interest to observe that profile (a) is not strictly consistent with the detailed asymptotic behavior defined by (4.2).] As noted earlier the data based on profile (c) agrees extremely well with the numerical calculations of Walker and Homsy [10]. The Weber values for Nu exceed those of the present analysis by about 14%.

Although Bejan's approach leads to closer agreement with the numerical and experimental results, it is apparent that the integral solutions also agree well with this data. Further, Bankvall's calculations for $L^{-1} = 7.5$ can be approximated by

$$Nu \approx 0.181\, R^{0.51} \tag{5.3}$$

for $R > 3000$. The Weber result, which is the asymptotic limit $R \to \infty$ of Bejan's analysis, gives

$$Nu \approx 0.212\, R^{0.5}, \tag{5.4}$$

whereas the present method yields

$$Nu \approx 0.186\, R^{0.5} \tag{5.5}$$

which compares favorably with (5.3). As noted earlier (see Table 2), the asymptotic limit (5.5) also agrees with the numerical solutions of Walker and Homsy [10]. These results show that the standard condition $\psi_z(0) = \psi_\infty(1) = 0$, together with an accurate method for integrating the boundary-layer equations, does lead to solutions which are compatible with the numerical and experimental data.

Acknowledgements—The authors are grateful to Professor G. M. Homsy for some helpful comments. This work was completed with support from the National Science Foundation under Grant No. ENG-7904045.

REFERENCES

1. M. A. Combarnous and S. A. Bories, Hydrothermal convection in saturated porous media, *Adv. Hydrosci.* **10,** 232 (1975).
2. D. T. J. Hurle, Hydrodynamics in crystal growth, *Current Topics in Material Science*, Vol. 2, p. 549. Elsevier, Amsterdam (1977).
3. J. E. Hart, Stability of thin non-rotating Hadley circulations, *J. Atmos. Sci.* **29,** 687 (1972).
4. J. W. Elder, Laminar free convection in a vertical slot, *J. Fluid Mech.* **23,** 77 (1965).
5. A. E. Gill, The boundary layer regime for convection in a rectangular cavity, *J. Fluid Mech.* **26,** 515 (1966).
6. G. F. Carrier, On the integration of equations associated with problems involving convection and diffusion, *Proceedings of the Tenth International Congress on Applied Mechanics*, Elsevier, Amsterdam (1962).
7. C. Quon, High Rayleigh number convection in an enclosure—A numerical study, *Physics Fluids* **15,** 12 (1972). See also comments by D. E. Cormack and L. G. Leal, *Physics Fluids* **17,** 1049 (1974).
8. C. Quon, Free convection in an enclosure revisited, *J. Heat Transfer* **99,** 340 (1977).
9. P. A. Blythe and P. G. Simpkins, Thermal convection in a rectangular cavity, *Physicochemical Hydrodynamics* (edited by D. B. Spalding), p. 511, Advance, New York (1977).
10. K. L. Walker and G. M. Homsy, Convection in a porous cavity, *J. Fluid Mech.* **87,** 449 (1978).
11. J. E. Weber, The boundary layer regime for convection in a vertical porous layer, *Int. J. Heat Mass Transfer* **18,** 569 (1975).
12. A. Bejan, Note on Gill's solution for free convection in a vertical enclosure, *J. Fluid Mech.* **90,** 561 (1979).
13. A. Bejan, On the boundary layer regime in a vertical enclosure filled with a porous medium, *Letters Heat Mass Transfer* **6,** 93 (1979).
14. M. Abramowitz and I. A. Stegun, *Handbook of Mathematical Functions*, Dover, New York (1965).
15. S. Klarsfeld, Champs de température associés aux movements de convection naturelle dans un milieu poreux limité, *Rev. Gén. Thermique* **9,** 1403 (1970).
16. C. G. Bankvall, Natural convection in vertical permeable space, *Wärme- und Stoffübertragung* **7,** 22 (1974).

CONVECTION DANS UNE COUCHE POREUSE

Résumé—On étudie les mouvements convectifs stationnaires dans une cavité rectangulaire emplie d'un matériau poreux, dans une large limite de nombre de Rayleigh, pour des écoulements gouvernés par un gradient horizontal de température. La structure de couche limite sur les parois est déterminée par une approche de relations intégrales. Cette méthode conduit à des résultats pour le flux massique principal, pour le gradient de température dans le coeur et pour le transfert thermique, résultats qui sont en excellent accord avec des solutions numériques des équations de la couche limite.

KONVEKTION IN EINER PORÖSEN SCHICHT

Zusammenfassung—Stationäre Konvektionsbewegungen in einem rechteckigen, mit porösem Material gefüllten Behälter wurden in dem großen Bereich der Rayleigh-Zahl für Strömungen, die durch einen horizontalen Temperaturgradienten verursacht werden, untersucht. Die Struktur der Grenzschicht an den Seitenwänden wurde durch Verwendung einer intergralen Näherungsbeziehung bestimmt. Diese Methode führt zu Resultaten für den Massenstrom, den Temperaturgradienten im Kern und für das Wärmeübertragungsverhalten, das sich in ausgezeichneter Übereinstimmung mit den numerischen Lösungen der Grenzschichtgleichungen befindet.

КОНВЕКЦИЯ В ПОРИСТОМ СЛОЕ

Аннотация — Исследуются устойчивые конвективные движения при больших числах Релея внутри прямоугольной заполненной пористым материалом полости для потоков, вызванных горизонтальным градиентом температуры. С помощью метода интегральных соотношений определена структура пограничного слоя на боковых стенках полости. Метод позволяет рассчитать поток массы и градиент температуры в ядре течения, а также характеристики теплообмена. Результаты хорошо согласуются с численными решениями уравнений пограничного слоя.